

---

Article

# Direct Bonding Method for Completely Cured Polyimide by Surface Activation and Wetting

Ying Meng<sup>1,2</sup>, Runhua Gao<sup>1,\*</sup>, Xinhua Wang<sup>1,2,3,\*</sup>, Sen Huang<sup>1,2,3</sup>, Ke Wei<sup>1</sup>, Dahai Wang<sup>1</sup>, Fengwen Mu<sup>4,\*</sup>, Xinyu Liu<sup>1,2</sup>

<sup>1</sup> High-Frequency High-Voltage Device and Integrated Circuits R&D Center, Institute of Microelectronics, Chinese Academy of Sciences, Beijing 100029, China

<sup>2</sup> University of Chinese Academy of Sciences, Beijing 100049, China

<sup>3</sup> Key Laboratory of Microelectronic Devices & Integrated Technology, Institute of Microelectronics, Chinese Academy of Sciences, Beijing 100029, China

<sup>4</sup> SABers Co., Ltd., Tianjing 300450, China

\* Correspondence: Fengwen Mu :mufengwen@saber-s.com; Runhua Gao: gao594730085@gmail.com

**Abstract:** Polymer adhesives have emerged as a promising dielectric passivation layer in hybrid bonding for 3D integration while they raise misalignment problems during curing. In this work, the synergistic effect of oxygen plasma surface activation and wetting is utilized to achieve bonding between completely cured polyimides. The optimized process achieves a void-less bonding with a maximum shear strength of 35.3 MPa at a low temperature of 250 °C in merely 2 min, significantly shortening the bonding period and decreasing thermal stress. It is found that the plasma activation generated hydrophilic groups on the polyimide surface, and the wetting process further introduced more -OH groups and water molecules on the activated polyimide surface. The synergistic process of plasma activation and wetting facilitates bridging polyimide interfaces to achieve bonding, providing an alternative path for adhesive bonding in 3D integration.

**Keywords:** polyimide bonding; plasma activation; hydrophilic; hybrid bonding; 3D integration

---

## 1. Introduction

The number of transistors on electronics was supposed to increase exponentially according to Moore's Law, while this trend became difficult to sustain in traditional two-dimensional integration due to the physical limits of transistor size, the high costs of processes, and the dependence on high-precision lithography equipment. Three-dimensional (3D) integration technology [1-4] has offered an alternate path to continue Moore's law. Through this technology, the chips or wafers with different functions are separately manufactured and vertically stacked through a hybrid bonding process, hence the significance of the hybrid bonding technology. Silicon dioxide (SiO<sub>2</sub>) is usually used to fill gaps between metal interconnections in traditional hybrid bonding, to prevent the metal from oxidation during the bonding process and increase the bonding area effectively. However, the SiO<sub>2</sub> surface is required high flatness and surface cleanliness to avoid electrical interconnection failure because of its higher hardness and poor deformation characteristics. Moreover, the mismatch of the coefficient of thermal expansion (CTE) between SiO<sub>2</sub> and the metal may generate residual stress during the bonding process and cause reliability issues. Adhesive possesses the advantages of flexible, higher surface roughness and flatness tolerance that can be used to replace oxides as a buffer layer to release residual stress from bonding pressure. Therefore, adhesive/metal hybrid bonding is a promising solution for 3D integration.

Typical hybrid bonding consists of metal/metal and adhesive/adhesive bonding; the former achieves electrical interconnection and the latter provides passivation protection and mechanical support. Most researchers achieve the hybrid bonding process by two steps, where they separately bond metals and adhesives [5-8], as shown in Figure 1 (a)

and (b). The “adhesive first” method benefits void-free and reliable adhesive bonding but raises serious misalignment of metal interconnection due to the fluidity and volume shrinkage of adhesives during the curing process. The “metal first” method avoids the misalignment problem, while the post-bonding curing process for adhesives causes out-gas and degrade bonding reliability. Either the “adhesive first” or the “metal first” is inevitable to involve a curing procedure in the bonding process, not only raising various problems but also increasing the bonding period. Many attempts have been made to cure adhesive completely before hybrid bonding [9,10], as shown in Figure 1(c). A high-quality dielectric passivation layer was achieved because the solvent and volatile substances of the adhesive can be removed completely. Among them, polyimide is a promising adhesive due to its advances in flexibility, chemical inertness, mechanical toughness, and thermal stability at high temperatures [11,12], which makes it withstands manufacturing processes such as metal deposition, photolithography, wet etching process. However, completely cured polyimides, due to their higher glass transition temperature [13], require higher bonding temperatures that are unsuitable for advanced application devices such as dynamic random access memory (DRAM) [14] and light emitting diode (LED) [15]. Therefore, it is necessary to develop a rapid and low-temperature (< 250°C) bonding method for completed cured polyimides to achieve bonding with high throughput and reliability.

Considerable research has been conducted on the adhesion between cured polyimides. Harutaka Mekar [16] bonded two pieces of polyimide films by thermo-compression method with a high temperature approaching the glass transition temperature, yet possible side effects of the high-temperature process still need discussion. Chih Chen et al. [17] bonded two pieces of polyimide films by heating at 250 °C for 60 min in an oven, finding that voids inevitably existed either at the bonding interface or within the bulk films. A modified surface activated bonding (mSAB) method was proposed to bond polyimides by a thin intermediate activated metallic layer, which is promising while the metallic layer may cause short circuit and failure when through-silicon-via technology is involved [18]. So far, it is still challenging to develop a low-temperature bonding method for ordinary polyimide to meet the requirements of low thermal budget, high throughput, and reliability. In the case of traditional wafer bonding, surface elastic deformation, hydrogen bond of -OH groups [19], and H<sub>2</sub>O molecular bridging [20] all play important roles in the wafer bonding. Additionally, previous studies that proved the synergistic effects of irradiation and ethanol on the bonding between polyimide and metal [21,22], demonstrating the hydrophilic group is the key to the bonding process. Inspired by the above reports, in this study, a novel bonding method utilizing the synergistic effects of oxygen plasma surface activation and wetting process is proposed. The polyimide surface was activated by oxygen plasma first, and the vertical bonding was achieved by thermo-compression in a nitrogen atmosphere. This method is promising to shorten the bonding process and elevate the throughput and efficiency. In this study, the oxygen plasma activation and H<sub>2</sub>O molecular bridge were introduced into the bonding process.

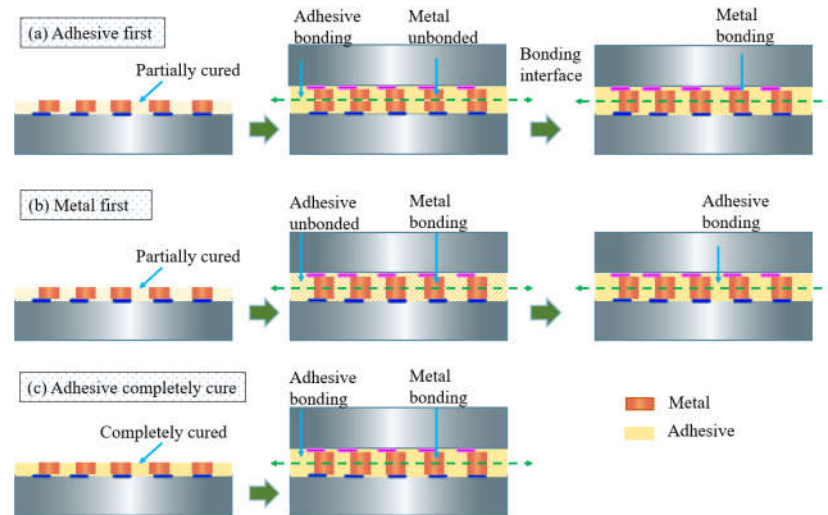


**Figure 1.** The schematic of hybrid bonding in 3D integration: (a) the adhesive first method, (b) the metal first method, (c) the method in this study.

## 2. Materials and Methods

The polyimide used in this study is synthesized from pyromellitic dianhydride and 4,4'-diaminodiphenyl ether (PMDA/4,4'-ODA), which was processed into films of 50  $\mu\text{m}$  by an advanced salivating biaxial stretching and was cut to 12 mm  $\times$  12 mm. The polyimide films were sequentially sonicated with acetone, alcohol, and deionized water for 5 minutes to remove pollution, then were dried with nitrogen and heated by a hotplate at 100°C for 10 min to remove the remaining moisture. The film surfaces were activated by reactive ion etching equipment (RIE; 100M, Tailong Electronics Co. Ltd.) using the oxygen plasma with 150 W power and 50 sccm oxygen flow. This activation aims to remove organic pollution and modify the surface to improve its hydrophilicity. Two pieces of activated polyimide films were stacked face to face with deionized water dropped at their interface, then were transformed into a thermo-compression chamber to achieve bonding in nitrogen under a pressure of 30 MPa. The stacked polyimide was heated from the bottom side, and pressure was applied on the top side by an aluminum block with an area of 6 mm  $\times$  6 mm to precisely control the effective bonding area.

The surface morphology of the polyimide films before and after surface activation was characterized by the atomic force microscope (AFM; XE15, Park systems Co. Ltd). The surface roughness was evaluated by the root mean square average ( $R_{\text{rms}}$ ) and average roughness ( $R_a$ ). Where, the  $R_{\text{rms}}$  is the roughness calculated based on the ordinary least squares method, which was obtained by the height deviations taken from the mean image data plane; the  $R_a$  is the arithmetic average of the absolute values of the surface height deviations measured from the mean plane. The calculation method is expressed as follows:

$$R_{\text{rms}} = \sqrt{\frac{\sum Z_m^2}{N}} \quad (1)$$

$$R_a = \frac{1}{N} \sum_{n=1}^N |Z_n| \quad (2)$$

Where  $Z_m(Z_n)$  is the height at position  $m(n)$ ,  $N$  denotes the number of data points for one direction. As the irradiation of plasma is reported to cause higher roughness, compensation through the elastic deformation of the near-surface area was considered for the interface gap caused by surface roughness [23,24]. The elastic energy must be smaller than the work of adhesion (namely, the interface energy gain by the bond formation) to achieve intimate contact, expressed as the formula (3) [25,26]:

$$\frac{R_{\text{rms}}^2}{\lambda} \leq \frac{2(1-\nu^2)}{\pi E} W_A \quad (3)$$

where,  $\lambda$  is the wavelength of the surface profile,  $E$  is Young's modulus,  $\nu$  is the Poisson's ratio,  $W_A$  is the work of adhesion.

In addition, the surface profile is also a crucial parameter that affects the bonding strength. In this study, the power spectral density (PSD) was statistical to reveal the periodic characteristic of wavelengths in the surface profile of samples, providing a distribution of features wavelengths from AFM profile data. The PSD represents the functional relationship between the magnitude of the surface roughness and spatial frequency (the inverse of the wavelength of the surface profile), as expressed as follows:

$$S_2(f_x, f_y) = \frac{1}{L^2} \left[ \sum_{m=1}^N \sum_{n=1}^N Z_{mn} e^{-2\pi i \Delta L (f_x m + f_y n)} (\Delta L)^2 \right] \quad (4)$$

where  $S_2$  represents the 2D-isotropic PSD of the surface,  $L$  is the length of the scanned area,  $N$  denotes the number of data points for one direction,  $Z_{mn}$  is the height at position  $(m, n)$ , and  $f_x$  and  $f_y$  express the spatial frequencies in the  $x$  and  $y$  directions, respectively. The surface morphology result was recorded in tapping mode by AFM and converted by Fourier transform, then the values were carried into formula (4) to extract the wavelength of the signal.

X-ray photoelectron spectroscopy (XPS; Thermo escalab 250Xi, Thermo Fisher Scientific Inc.) and Fourier infrared spectrometer (FTIR; Nicolet IS10, Thermo Fisher Scientific Inc.) were used to evaluate the chemical state of the polyimide surface before and after plasma irradiation. The emission angle of X-ray collection electrons was set as  $40^\circ$ . For the bonding strength test, the upper and lower sides of the bonded polyimides were glued with aluminum blocks using acrylic glue, and shear tests were conducted on the blocks by a shear tester (MFM 1200, TRY Precision Co. Ltd) with a shear speed of  $20 \mu\text{m/s}$ . In addition, cross-sectional samples were prepared by embedding the bonded polyimide in resin and cutting them using a focused ion beam (FIB; Helios G4, Thermo Fisher Scientific Inc.). The bonding interface was observed with a transmission electron microscope (TEM; Themis Z, FEI Inc.).

### 3. Results and discussion

#### 3.1. Process optimization

As bonding strength is a primary indicator to evaluate the reliability of vertical interconnections, the bonding process was optimized based on shear tests. The influence of volume of the introduced water, bonding time, plasma activation time, and bonding temperature on shear strength is shown in Figure 2. First, the oxygen plasma activation was set to 150 W, 180 s, and deionized water was dropped at the polyimide surfaces with different volumes (0.5 - 2.5  $\mu\text{L}$ ). The bonding temperature, the bonding time, and the pressure were decided to be  $250^\circ\text{C}$ , 600 s, and 30 MPa, respectively. The influence of the water volume on shear strength is shown in Figure 2(a). It is seen that the shear strength slightly changed with different volumes of induced water, and 1  $\mu\text{L}$  water appears a little superior. For the following experiments, the water volume was fixed at 1.0  $\mu\text{L}$ .

The influence of bonding time on shear strength is shown in Figure 2(b), where the oxygen plasma time, the bonding temperature, and the pressure were decided to be 180s,  $250^\circ\text{C}$ , and 30 MPa, respectively. The average shear strength was as high as 25 MPa even after bonding for merely 120 s and was slightly improved when the bonding time increased to 600 s. Although the bonding time is generally believed to positively correlate to the bonding quality, in this study, the bonding time of 120 s already obtained sufficient shear strength that meets the requirements of reliability.

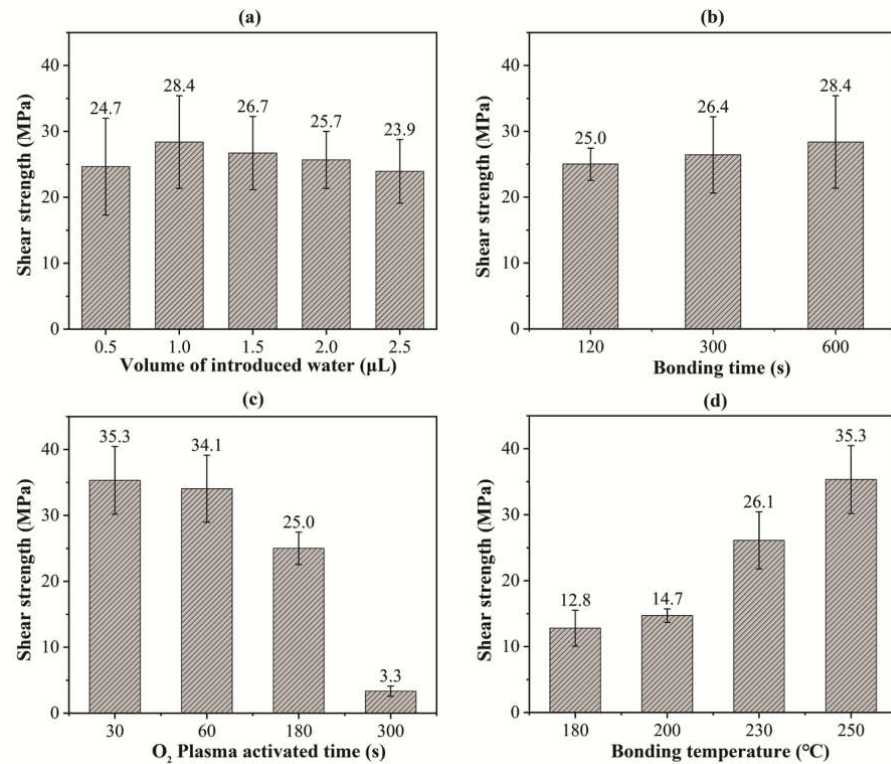


**Figure 2.** Shear strength of the polyimide bonding with different (a) water volume, (b) bonding time, (c) plasma activation time, and (d) temperatures.

As plasma activation time increased the surface roughness, it is necessary to analyze the effect of extending plasma time on the shear strength. The bonding time and temperature were set to 120 s and 250 °C, and polyimides were bonded after irradiating for 30 s, 60 s, 180 s, and 300 s with 150 W power and 50 sccm oxygen flow, and results are shown in Figure 2(c). The average shear strength, which has met the requirement, hardly changed with extending plasma activation when the time was less than 60 s. When the activated time was extended to 180 s, the shear strength decreased slightly and became unstable. Especially, when the time extended to 300 s, the shear strength greatly decreased to the extent of failure. Therefore, in this study, the plasma activation time was optimized to 30 s.

Then, the bonding time was fixed at 120 s and the oxygen plasma time was fixed at 30 s. The bonding temperature was adjusted to 180 °C, 200 °C, 230 °C, 250 °C, and results are shown in Figure 2(d), which obviously shows the positive correlation between the bonding temperature and the shear strength. Under the bonding temperature of 180 °C, the polyimide has been successfully bonded together with a shear strength of 12.8 MPa. The average shear strength reached the maximum of 35.3 MPa under the temperature of 250 °C. This correlation is reasonable because a higher bonding temperature accelerates the thermal vibration of atoms, making it easier to leave the equilibrium position and diffuse, and obtaining an interface with higher shear strength.

Additionally, the synergistic effects of plasma activation and deionized water molecular on the shear strength were proved by comparative tests, as listed in Table 1, and the corresponding shear strength is shown in Figure 3(a). The inserted images exhibit the specimens after bonding under different conditions, and the well-bonded areas appear dark. The specimens bonded without oxygen plasma activation and wetting (group #1) possessed the lowest shear strength and the smallest bonding area. This situation was not significantly improved by merely introducing water molecules on the surface (group #2),

while the bonding area has been slightly improved. Although the plasma activation process of group #3 increased both the bonding area and the shear strength, it failed to obtain a high shear strength. The process of group #4, which introduced both the water molecule and oxygen plasma activation, obtained bonding with not only a full bonding area but also a high shear strength. The bonding interfaces observed by the TEM, as shown in Figure 3(b), confirm voids exist neither in the inner polyimides nor at the bonding interface in both cases of groups #3 and #4; while a more compact bonding with a narrower bondline is observed for group #4. The results prove the positive synergistic effects of water molecules and oxygen plasma activation, which thickened the transition zone to ~10 nm. Therefore, it is proved that the synergy of oxygen plasma activation and water molecule is essential for high-quality polyimide-polyimide bonding.

**Table 1.** Comparative tests with or without plasma activation and water molecule assisting.

Group	O2 plasma activation	H2O
#1	×	×
#2	×	√
#3	√	×
#4	√	√

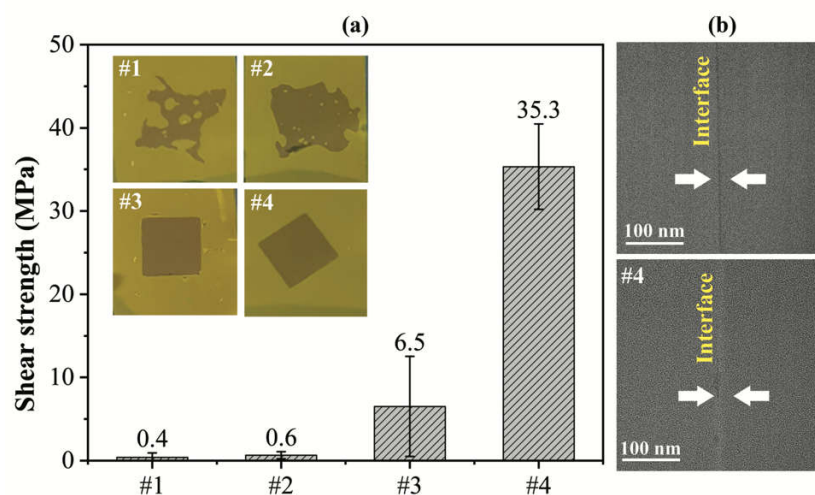


**Figure 3.** The shear strength of specimens obtained in the comparative tests of Table 1; the inserted images show the specimens after bonding under different conditions.

### 3.2. Effects of oxygen plasma activation on the polyimide surface

The oxygen plasma activation is supposed to raise the hydrophilicity of the polyimide and its effects are evaluated by the water-drop test. Deionized water was dropped on the polyimide surface after plasma activation of 0 s, 30 s, 60 s, 180 s, and 300 s, and the contact angles between the droplets and the surface were fit semi-automatically by capturing a picture, as shown in Figure 4(a). The contact angle of polyimide before plasma activation was  $79.67^\circ$ , indicating the poor hydrophilicity of polyimide. The hydrophilicity was significantly improved after plasma activation of over 30 s, as the contact angle greatly decreased to below the measurement limit ( $10^\circ$ ). A further extending activation time barely changed the contact angles.

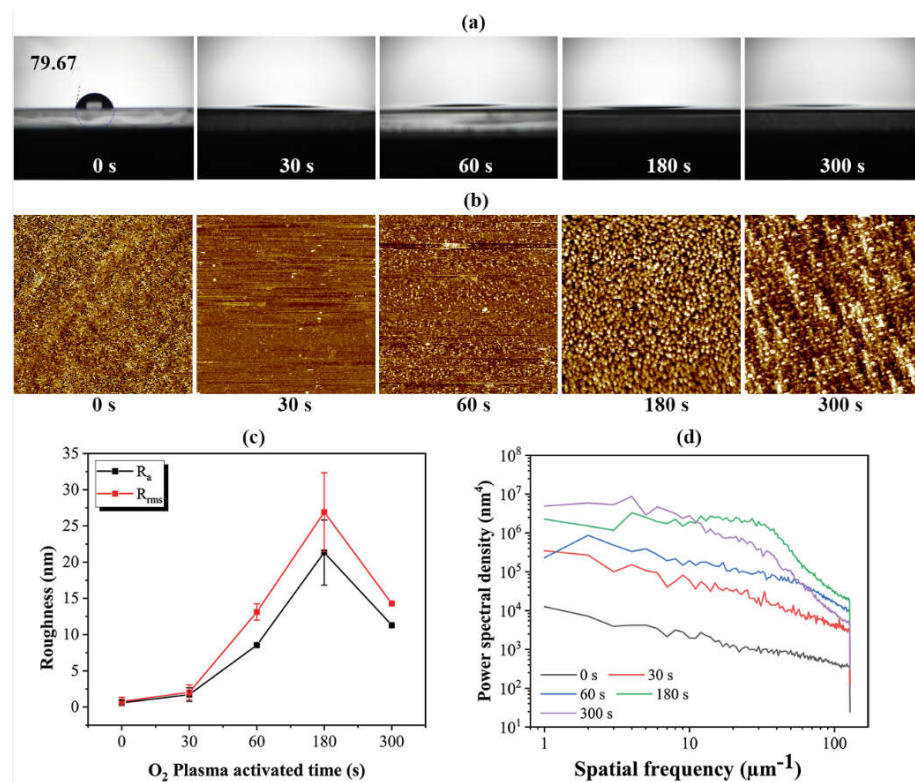


**Figure 4.** (a) contact angle, (b) AFM results, (c)  $R_{rms}$  and  $R_a$  roughness, and (d) power spectral density of the polyimide surface after plasma activation of different period.

Additionally, the surface morphology and their corresponding average surface roughness greatly changed when activation time varied. Both  $R_{rms}$  and  $R_a$  increased dramatically with extending activation time, until the activation time exceeded 180 s, the roughness decreased instead, as shown in Figure 4(c). The roughness comes from the surface texture such as uneven “hillocks”, thus it is considered that extending plasma time caused the increase of surface roughness by raising the amplitude of hillocks on the surface, while the decrease of that at 300 s may be explained by the PSD test. The PSD results of polyimide surfaces with different activation time are shown in Figure 4(d), which reveals the number of hillocks with different spatial frequency. The PSD curves are approximately parallel and rise equally when activation time increase from 0 to 180 s, suggesting the plasma irradiation not only increased the amplitude of hillocks but also raised the number of hillocks in all size. After irradiation for 180 s, the hillocks with spatial frequency from 30 to 60  $\mu\text{m}^{-1}$  increased significantly, namely the hillocks with middle size greatly formed, which also can be observed in Figure 4(b). When the activation time further extended to 300 s, the number of hillocks with spatial frequency less than 10  $\mu\text{m}^{-1}$  still raised significantly, while that above 10  $\mu\text{m}^{-1}$  became even lower because nanosize hillocks started to agglomerate under plasma irradiation, producing many larger micro hillocks. It is considered that the texture on the bonding surfaces greatly affected the bonding quality, because the shear strength obviously decreased when micro-hillocks formed on the surface when activated time extended to 180 and 300 s, as shown in Figure 4(c). These micro hillocks are believed to reduce actual contact area and create gaps that hindered atom diffusion, eventually causing debonding.

XPS and FTIR were used to further analyze the modification functional groups of polyimide surface. The angular-resolved XPS with high-resolution accuracy was used to quantitatively verify the changes in the elements and functional groups before and after the plasma activation. The emission angle of X-ray collection electrons was set as 40° to detect elements and chemical bonds of polyimide surface. The C 1s, N 1s, and O 1s spectra

of polyimide before and after plasma activation are shown in Figure 5(a). The C 1s spectrum is deconvoluted into four components: C-C(C-H) in ODA at 284.8 eV, C-N in ODA and C-C(C-H) in PMDA at 285.3 eV, C-O in ODA at 286.1 eV, C=O in PMDA at 288.6 eV. The N 1s spectrum is deconvoluted into two components: the C-N-C in PMDA at 400.4 eV and C-N-H in PMDA at 398.5eV. The O 1s spectrum is deconvoluted into two components: the O-C in ODA at 533.2eV and the O=C in PMDA at 531.0 eV. After plasma treatment, as the rough comparison between the two spectra, the total content of C element decreased, while that of O and N elements increased obviously. For ease of understanding, the XPS results of polyimide after activation are respectively explained by element spectrum, as addressed as follows: (I) In C 1s spectrum, the ratio of the C-C and C-C/C-N bond decreased, while that of the C-O and C=O bond increased after the oxygen plasma activated. Moreover, a new hydrophilic group of C-OH bond at 287 eV emerged. (II) In the N1s spectrum, the ratio of C-N-C bond decreased, and C-N-H bond increased. This reveals that oxygen plasma breaks the bonds of the long-chain molecule to become short-chain molecules on the polyimide surface. (III) In the O 1s spectrum, the ratio of C-O bond increased, and that of the C-O to C=O bond was 1.72, which approached to the ratio of the (C-O + C-OH) to C=O (1.62), as shown in C1s spectrum in Figure 5(b). Therefore, the composition of C-O-C in the O 1s spectrum contains two parts: C-O bond in ODA and the new C-OH bond.

In addition, the FTIR results of the polyimide before and after plasma activation are shown in Figure 5(c) and Figure 5(d). In both samples, the C=O bending in imide ring at 720  $\text{cm}^{-1}$ , the C-O-C stretching and C-O-C asymmetrical at 1013  $\text{cm}^{-1}$  and 1231  $\text{cm}^{-1}$ , the C-N stretching at 1360  $\text{cm}^{-1}$ , the aromatic C=C ring stretch at 1495  $\text{cm}^{-1}$ , the C=O asymmetrical stretching and C=O symmetrical stretching at peak of 1709  $\text{cm}^{-1}$  and 1775  $\text{cm}^{-1}$  were detected. The area of C=O symmetrical stretching at 1775  $\text{cm}^{-1}$  and the C-O-C stretching at 1231  $\text{cm}^{-1}$  and 1013  $\text{cm}^{-1}$  slightly increased after the plasma activation compared to functional group as-receive, while the area of imide ring at 720 $\text{cm}^{-1}$  and the C-N stretching 1360  $\text{cm}^{-1}$  decreased. These results indicate that the oxygen plasma broke the bond of C-N-C and the imide ring, and reacted with the polyimide to produce new hydrophilic groups such as C=O and C-O. The results are consistent with the previously reported [27,28] that oxygen plasma will break the imide rings and phenyl groups at the surface of polyimide film. Moreover, new OH groups were detected on the polyimide surface after plasma activation and wetting process, as highlighted by the red circle in Figure 5(d), and the surface after wetting also exhibit higher C-O-C and OH signals.

In general, the XPS results show that the oxygen plasma tended to break C-C, C-N bonds while was beneficial to the formation of C-O and C=O groups on the polyimide surface, and these results well match with FTIR results. A schematic of polyimide surface activation and wetting bonding method is illustrated in Figure 6. The oxygen plasma activation introduces low-density hydrophilic groups on the polyimide surface, effectively enhancing the adsorption of water molecules, which brings considerable high-density OH groups. Firstly, the adsorbed water molecules facilitate the generation of a pre-bonding at the bonding interfaces [29]; moreover, the considerable hydrophilic groups on the surface benefit to generate bridging bonds between polyimides, which provide a compact contact of atoms. Such compact contact promotes the generation of stable covalent bonds under appropriate bonding time and pressure, hence the improvement in bonding quality. This synergistic effect explains the results in Figure 3, that neither the plasma activation nor the hydration method is sufficient to achieve satisfied bonding alone. A reliable polyimide/polyimide bonding provides mechanical support and protection for metal interconnection, and simplifies the semiconductor processing in subsequent manufactures.

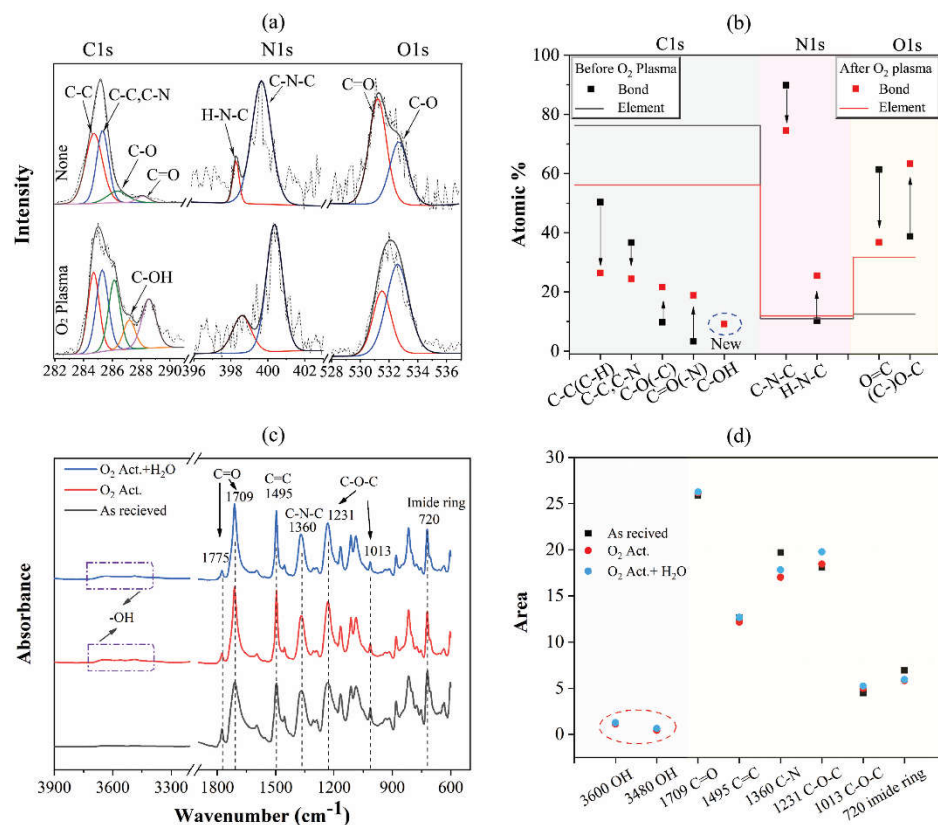


**Figure 5.** The status of polyimide surfaces before and after the plasma activation: (a) C 1s, N 1s, O 1s core-level XPS spectra; (b) the ratio of the functional groups; (c) the infrared absorption spectrum obtained via FTIR tests; (d) the area of feature functional groups in spectral. Act.: activation.

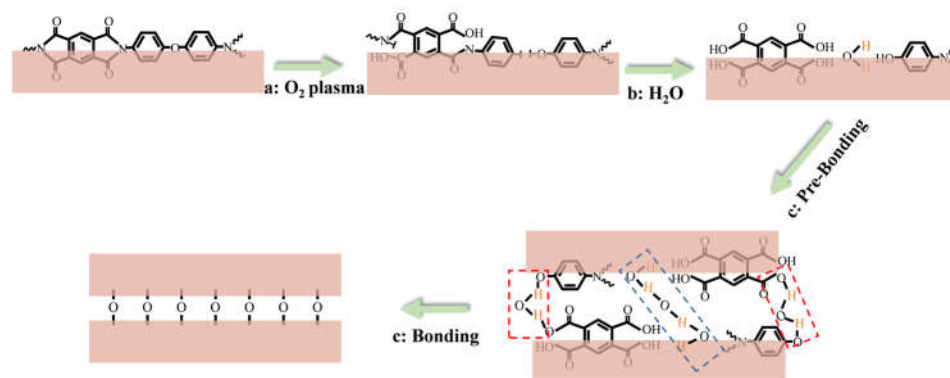


**Figure 6.** The schematic of polyimide surface activation and wetting bonding method.

#### 4. Conclusions

In summary, completely cured polyimides are directly bonded by the process involving O<sub>2</sub> plasma activation and wetting procedures. By the optimized process, polyimide/polyimide bonding with a high shear strength of 35.3 MPa was achieved in 2 min at 250°C and under a pressure of 30 MPa. The synthetic effect of oxygen plasma activation and wetting molecular has been proven to promote the high-quality bonding interface between the polyimides. It is found that the oxygen plasma breaks the long-chain molecules into short-chain molecules and creates hydrophilic groups, with that the adsorbed water introduces considerable hydrophilic groups with high-density bridging at interfaces, thus the bonding is promoted. However, long-time plasma activation will generate micro hillocks that increase surface roughness, hindering bonding in return. The proposed

bonding process shortens the bonding period and increases the bonding strength significantly, and is promising for 3D integration processes. Importantly, although the proposed process was investigated for the polyimide/polyimide interface, this study revealed the possibility of scaling the mechanism to other polymer dielectric passivation layers such as PEEK, PMMA, etc.

**Author Contributions:** conceptualization, methodology, writing, Ying Meng; methodology, resources, writing, Runhua Gao; investigation, validation, Xinhua Wang; visualization, Sen Huang; methodology, resources, Ke Wei; methodology, resources, Dahai Wang; validation, supervision, Fengwen Mu; project administration, Xinyu Liu.

**Data Availability Statement:** Not applicable.

**Acknowledgments:** This work was supported in part by National Natural Science Foundation of China under Grant 62004213, Grant 61527816, Grant 11634002, Grant 61631021, Grant 62074161, Grant 61822407, Grant 52105416 and Grant U20A20208; in part by the Key Research Program of Frontier Sciences, Chinese Academy of Sciences (CAS) under Grant QYZDB-SSW-JSC012; in part by the Youth Innovation Promotion Association of CAS; in part by the University of CAS; and in part by the Opening Project of Key Laboratory of Microelectronic Devices & Integrated Technology, Institute of Microelectronics, CAS.

**Conflicts of Interest:** The authors declare no conflict of interest.

## References

1. Liu, F.; Yu, R. R.; Young, A. M.; Doyle, J. P.; Wang, X.; Shi, L.; Chen, K. N.; Li, X.; Dipaola, D. A.; Brown, D.; Ryan, C. T.; Hagan, J. A.; Wong, K. H.; Lu, M.; Gu, X.; Klymko, N. R.; Perfecto, E. D.; Merryman, A. G.; Kelly, K. A.; Purushothaman, S.; Koester, S. J.; Wisnieff, R.; Haensch, W. A 300-mm wafer-level three-dimensional integration scheme using tungsten through-silicon via and hybrid Cu-adhesive bonding[C]//2008 IEEE International Electron Devices Meeting. IEEE, 2008, 1-4. [[CrossRef](#)].
2. Topol, A. W.; La Tulipe, D. C.; Shi, Jr, L.; Frank, D. J.; Bernstein, K.; Steen, S. E.; Kumar, A.; Singco, G. U.; Young, A. M.; Guarini, K. W.; Ieong, M. Three-dimensional integrated circuits[J]. IBM Journal of Research and Development, 2006, 50(4.5), 491-506. [[CrossRef](#)].
3. Enquist, P.; Fountain, G.; Petteway, C.; Hollingsworth, A.; Grady, H. Low cost of ownership scalable copper direct bond interconnect 3D IC technology for three dimensional integrated circuit applications[C]//2009 IEEE International Conference on 3D System Integration. IEEE, 2009, 1-6. [[CrossRef](#)].
4. Peng, L.; Zhang, L.; Fan, J.; Li, H. Y.; Lim, D. F.; Tan, C. S. Ultrafine Pitch (6  $\mu\text{m}$ ) of Recessed and Bonded Cu-Cu Interconnects by Three-Dimensional Wafer Stacking. IEEE electron device letters, 2012, 33(12), 1747-1749. [[CrossRef](#)].
5. Sakai, T.; Imaizumi, N.; Sakuyama, S. Hybrid bonding technology with Cu-Cu/adhesives for high density 2.5 D/3D integration. Proc. Tech. Program Pan Pac. Microelectron. Symp. 2016, 1-6. [[CrossRef](#)].
6. He, R.; Fujino, M.; Akaike, M.; Sakai, T.; Sakuyama, S.; Suga, T. Cu/Adhesive hybrid bonding at 180° C in H-containing HCOOH vapor ambient for 2.5 D/3D integration. IEEE Electron. Compon. Technol. Conf. 2017, 1243-1248. [[CrossRef](#)].
7. Huang, Y. J.; Chen, H. C.; Yu, T. Y.; Lai, B. H.; Shih, Y. C.; Chen, K. N. Asymmetry hybrid bonding using Cu/Sn bonding with polyimide for 3D heterogeneous integration applications. International Microsystems, Packaging, Assembly and Circuits Technology Conference. 2017, 187-190. [[CrossRef](#)].
8. Yao, M.; Zhao, N.; Wang, T.; Yu, D.; Xiao, Z.; Ma, H. Study of three-dimensional small chip stacking using low cost wafer-level micro-bump/B-stage adhesive film hybrid bonding and via-last TSVs. J. Electron. Mater. 2018, 47(12). 7544-7557. [[CrossRef](#)].
9. Lu, C. H.; Kho, Y. T.; Cheng, C. A.; Huang, Y. J.; Chen, K. N. Polymer for wafer-level hybrid bonding and its adhesion to passivation layer in 3D integration. International Conference on Electronics Packaging. 2017, 519-521. [[CrossRef](#)].
10. Yoneda, S.; Adachi, K.; Kobayashi, K.; Matsukawa, D.; Sasaki, M.; Itabashi, T.; Shibata, T. A Novel Photosensitive Polyimide Adhesive Material for Hybrid Bonding Processing. IEEE Electron. Compon. Technol. Conf. 2021, 680-686. [[CrossRef](#)].
11. Itabashi, T.; Kotani, M.; Zussman, M. P.; Zoschke, K.; Fischer, T.; Töpfer, M.; Ishida, H. High temperature bonding solutions enabling thin wafer process and handling on 3D-IC manufacturing. IEEE International 3D Systems Integration Conference. 2011, 1-4. [[CrossRef](#)].
12. Lu, C. H.; Kho, Y.T.; Yang, Y.T.; Chen, Y.P.; Chen, C.P.; Hung, T.T.; Chen, C.F.; Chen, K.N. Adhesion Property of Polyimide and Passivation Layer for Polymer/metal Waferlevel Hybrid Bonding in 3D Integration. 68th Electronic Components and Technology Conference. 2018, 401-406. [[CrossRef](#)].
13. Yao, M.; Yu, D.; Zhao, N.; Fan, J.; Xiao, Z.; Ma, H. Development of wafer level hybrid bonding process using photosensitive adhesive and Cu pillar bump. China Semiconductor Technology International Conference. 2017, 1-3. [[CrossRef](#)].
14. Kim, Y. I.; Yang, K. H.; Lee, W. S. Thermal degradation of DRAM retention time: Characterization and improving techniques. IEEE International Reliability Physics Symposium. Proceedings. 2004, 667-668. [[CrossRef](#)].

15. Ko, C. T.; Chen, K. N. Low temperature bonding technology for 3D integration. *Microelectron. Reliab.* 2012, 52(2) 302-311. [[CrossRef](#)]
16. Mekaru, H. Thermal bonding of polyimide to form sealed microchannels." *Japanese Journal of Applied Physics.* 2017, 56.6S1, 06GM04. [[CrossRef](#)]
17. Liu, H. C.; Chen, C. Low temperature polyimide-to-polyimide direct bonding[C]//2019 6th International Workshop on Low Temperature Bonding for 3D Integration (LTB-3D). *IEEE*, 2019: 75-75. [[CrossRef](#)]
18. Matsumae, T.; Fujino, M.; Suga, T. Novel sealing technology for organic el display and lighting by means of modified surface activated bonding method[C]//2014 IEEE 64th Electronic Components and Technology Conference (ECTC). *IEEE*, 2014: 1504-1508. [[CrossRef](#)]
19. Grundner, M.; Jacob, H. Investigation of hydrophilic and hydrophobic silicon (100) wafer surfaces by X-ray photoelectron and high-resolution electron energy loss spectroscopy. *Appl. Phys. A*, 1986, 39, 73-82. [[CrossRef](#)]
20. Stengl R.; Tan T.; and Gosele. U. A model for silicon wafer bonding process. *Jpn. J. Appl. Phys.*, 1989, 28, 1735-1741. [[CrossRef](#)]
21. Yang, H. W.; Kao, C. R.; Shigetou, A. Fast Atom Beam and Vacuum-Ultraviolet-Activated Sites for Low-Temperature Hybrid Integration. *Langmuir.* 2017, 33(34), 8413-8419. [[CrossRef](#)]
22. Yang, T. H.; Yang, C. Y.; Shigetou, A.; Kao, C. R. A Single Process for Homogeneous and Heterogeneous Bonding in Flexible Electronics : Ethanol-Assisted Vacuum Ultraviolet (E-VUV) Irradiation Process. *International Conference on Electronics Packaging.* 2019, 117-122. [[CrossRef](#)]
23. Nakamura, Y.; Suzuki, Y.; Watanabe, Y. Effect of oxygen plasma etching on adhesion between polyimide films and metal. *Thin Solid Films* 290 (1996): 367-369. [[CrossRef](#)]
24. Kim, Y. J.; Byun, T. J.; Kim, S. I.; Han, J. G. Modification of the surface structure and properties of polymers fabricated by using an inductively coupled plasma. *Journal of the Korean Physical Society.* 2008, 53.3, 1401-1405. [[CrossRef](#)]
25. Takagi, H.; Maeda, R.; Chung, T. R.; Hosoda, N.; Suga, T. Effect of Surface Roughness on Room-Temperature Wafer Bonding by Ar Beam Surface Activation, *Jpn. J. Appl. Phys.* 1998, 37, pp.4197-4203. [[CrossRef](#)]
26. Itoh, T.; Suga, T. Necessary load for room temperature vacuum sealing, *J. Micromech. Microeng.* 2005, 15, S281-S285. [[CrossRef](#)]
27. Lei, H.; Zhang, M.; Niu, H.; Qi, S.; Tian, G.; Wu, D. Multilevel structure analysis of polyimide fibers with different chemical constitutions. *Polymer.* 2018, 149, 96-105. [[CrossRef](#)]
28. Kim, S.H.; Na, S.W.; Lee, N.E.; Nam, Y.W.; Kim, Y.H. Effect of surface roughness on the adhesion properties of Cu/Cr films on polyimide substrate treated by inductively coupled oxygen plasma, *Surf. Coat. Technol.* 2005, 200, 2072-2079. [[CrossRef](#)]
29. Xu, F.; Xue, T.; Liang, X.; Tan, Q. High-temperature direct bonding of langasite using oxygen plasma activation. *Scr. Mater.* 2021, 194, 113681. [[CrossRef](#)]